Two complementary molecular energy decomposition schemes: The Mayer and Ziegler–Rauk methods in comparison

Sergei F. Vyboishchikov,[1,a),b)] Andreas Krapp,[2,3,a),c)] and Gernot Frenking[2,a),d)]
[1]*Institut de Química Computacional, Campus de Montilivi, Universitat de Girona, 17071 Girona, Catalonia, Spain*
[2]*Fachbereich Chemie der Philipps-Universität Marburg, Hans-Meerwein-Str., 35032 Marburg, Germany*
[3]*Senter for Teoretisk og Beregningsorientert Kjemi, Kjemisk Institutt, Universitetet i Oslo, Postboks 1033 Blindern, 0315 Oslo, Norway*

(Received 18 June 2008; accepted 3 September 2008; published online 14 October 2008)

In the present paper we discuss and compare two different energy decomposition schemes: Mayer's Hartree–Fock energy decomposition into diatomic and monoatomic contributions [Chem. Phys. Lett. **382**, 265 (2003)], and the Ziegler–Rauk dissociation energy decomposition [Inorg. Chem. **18**, 1558 (1979)]. The Ziegler–Rauk scheme is based on a separation of a molecule into fragments, while Mayer's scheme can be used in the cases where a fragmentation of the system in clearly separable parts is not possible. In the Mayer scheme, the density of a free atom is deformed to give the one-atom Mulliken density that subsequently interacts to give rise to the diatomic interaction energy. We give a detailed analysis of the diatomic energy contributions in the Mayer scheme and a close look onto the one-atom Mulliken densities. The Mulliken density ρ^A has a single large maximum around the nuclear position of the atom A, but exhibits slightly negative values in the vicinity of neighboring atoms. The main connecting point between both analysis schemes is the electrostatic energy. Both decomposition schemes utilize the same electrostatic energy expression, but differ in how fragment densities are defined. In the Mayer scheme, the electrostatic component originates from the interaction of the *Mulliken* densities, while in the Ziegler–Rauk scheme, the *undisturbed* fragment densities interact. The values of the electrostatic energy resulting from the two schemes differ significantly but typically have the same order of magnitude. Both methods are useful and complementary since Mayer's decomposition focuses on the energy of the finally formed molecule, whereas the Ziegler–Rauk scheme describes the bond formation starting from undeformed fragment densities. © *2008 American Institute of Physics*. [DOI: 10.1063/1.2989805]

I. INTRODUCTION

The strength or the energy of the chemical bond is a central notion in chemistry. Most frequently, it is measured by the bond dissociation energy, since it can be both determined experimentally and calculated using quantum-chemical techniques. In order to calculate the dissociation energy of a molecule AB it is necessary to evaluate the energy difference $E(AB)-E(A)-E(B)$, where A and B are well-defined molecular fragments. However useful, the dissociation energy does not carry direct chemical information. In order to characterize interactions between the fragments, a number of energy partitioning methods[1,2] have been developed. The aim of these methods is to divide the total dissociation energy into physically meaningful components, which often allows deep understanding of the origin of the corresponding interaction.

An energetic characterization of a bond can be most easily performed by energy partitioning methods such as Kitaura–Morokuma or Ziegler–Rauk schemes[1,2] [the latter is conventionally referred to as energy decomposition analysis (EDA)], which turned out to be extremely useful. Note that we use the terms "partitioning" and "decomposition" synonymously. In these schemes, the total dissociation energy D_e is decomposed into a number of physically meaningful components by dividing the interaction process between two (or more) fragments A and B in a number of *gedanken* steps.

$$-D_e = E_{\text{int}} + E_{\text{prep}} = \Delta E_{\text{elstat}} + \Delta E_{\text{Pauli}} + \Delta E_{\text{orb}} + E_{\text{prep}}, \tag{1a}$$

$$-D_e = E_{\text{int}} + E_{\text{prep}} = \Delta E_{\text{elstat}} + \Delta E_{\text{ex}} + \Delta E_{\text{pol}} + \Delta E_{\text{CT}} + \Delta E_{\text{mix}} + E_{\text{prep}}. \tag{1b}$$

In the first step of the Ziegler–Rauk [Eq. (1a)] and the Kitaura–Morokuma scheme [Eq. (1b)] the fragments are geometrically deformed from their equilibrium geometry to their geometries in the final complex. The associated energy change is referred to as *preparation energy* E_{prep}. The total relaxation of the prepared fragments forming the final molecule is summed into the interaction energy term E_{int}. This term is further subdivided into three components. The ΔE_{elstat}

a)Author to whom correspondence should be addressed.
b)Electronic mail: vybo@iqc.udg.es. FAX: +34-972-418-356.
c)Electronic mail: andreas.krapp@kjemi.uio.no.
d)Electronic mail: frenking@chemie.uni-marburg.de. FAX: +49-6421-282-5566.

term is calculated as the classical electrostatic energy between the two prepared fragments superimposed with their frozen charge distribution at the geometry of the complex and is the same for both the Ziegler–Rauk and the Kitaura–Morokuma schemes.

In the Ziegler–Rauk analysis, the next step consists in the transformation from the superposition of the undisturbed wave functions Ψ^A and Ψ^B of the isolated fragments A and B to the wave function that obeys the Pauli principle. This wave function results from explicit antisymmetrization and renormalization of the product wave function: $\Psi^\circ(AB) = N\hat{A}[\Psi^A\Psi^B]$. The associated change in energy is referred to as Pauli repulsion energy ΔE_{Pauli}. The last component in the Ziegler–Rauk scheme is the orbital interaction ΔE_{orb}, which accounts for charge transfer (i.e., donor-acceptor interactions between occupied orbitals on one moiety and unoccupied orbitals of the other), polarization (empty/occupied orbital mixing on the same fragment due to the presence of another fragment), and electron-pair bonding (the stabilization arising from the formation of the electron-pair bonding configuration in which the bonding combination between the singly occupied molecular orbitals is formed and doubly occupied).

The electrostatic term in Eq. (1a) ΔE_{elstat} is defined as follows:

$$\Delta E_{\text{elstat}} = \frac{Z_A Z_B}{R_{AB}} - \int \frac{Z_B}{r_B}\rho^A(\mathbf{x})d\mathbf{x} - \int \frac{Z_A}{r_A}\rho^B(\mathbf{x})d\mathbf{x} + \int\int \frac{\rho^A(\mathbf{x})\rho^B(\mathbf{x}')}{|\mathbf{r}-\mathbf{r}'|}d\mathbf{x}d\mathbf{x}'. \quad (2)$$

It comprises the nuclear repulsion (the first term), the electron-nuclear attraction (the second and the third term), and the electron-electron repulsion (the last term). The densities and ρ^A and ρ^B in Eq. (2) are the frozen charge densities of the fragments. Normally this contribution is stabilizing even in the case of neutral fragments as was analyzed in detail, e.g., in Ref. 3. For the Pauli repulsion term ΔE_{Pauli} and the orbital relaxation term ΔE_{orb} there is no simple way to write down the defining equation, but splitting ΔE_{Pauli} into potential and kinetic energy contributions has given useful insight.[4] It turns out that the antisymmetrization and renormalization of the product wave function lead to a depletion of charge from the overlap area between the fragments into the region near the nuclei. This charge depletion is a stabilizing contribution to the potential energy, but since this process also strongly increases the kinetic energy of the electrons, the overall result is the destabilization (positive energy contribution).

In the Kitaura–Morokuma analysis, the energy components are determined by the change in the total energy when well-defined interaction matrix elements are eliminated from the Fock and overlap matrices in a series of calculations. The electrostatic term was already discussed above. The exchange component (E_{ex}) describes the interaction between the occupied orbitals of fragment A and the occupied orbitals of fragment B that causes electron delocalization between the occupied orbitals of the two fragments. The polarization interaction (E_{pol}) is caused by mixing of occupied and virtual orbitals within each fragment. The charge-transfer interaction (E_{CT}) covers the interfragment delocalization by mixing occupied orbitals of one fragment with virtual orbitals of another fragment, and vice versa. The remaining interaction energy, which is calculated from the completely relaxed wave function and not covered by any of the above terms, is called E_{mix}. The Kitaura–Morokuma analysis allows to consider charge-transfer and polarization contributions separately, which has been proven to be useful for the interpretation of hydrogen bonding.[5] A drawback of the Kitaura–Morokuma scheme is that all components are obtained from wave functions that have not been antisymmetrized and thus do not satisfy the Pauli exclusion principle. Another problem is that the calculation of the polarization contribution is subject to the basis-set superposition error and that the error even increases with a larger basis set.[6] On the other hand, the Ziegler–Rauk scheme explicitly calculates the energy required for the antisymmetrization, but does not allow to split the orbital interaction term (ΔE_{orb}) further into charge-transfer and polarization contributions. The latter can be estimated by an additional calculation, in which the virtual orbitals of one fragment are deleted. A very nice feature of the Ziegler–Rauk scheme is the possibility of splitting ΔE_{orb} into contributions according to irreducible representations of the point group of the interacting system.

In some cases it is not possible or reasonable to separate a molecule into fragments. This is true, for example, when the bonds form a part of a ring system, or for weak intramolecular interactions, such as intramolecular hydrogen or agostic bonds. Hence, the question about the strength of such intramolecular interaction must be addressed by other means. Some insights about the bond strength are provided by Bader's atoms-in-molecules theory[7] and by the natural bond orbital (NBO) analysis.[8] Albeit very useful, these approaches do not yield a direct energetic measure of bond strength. It should be noted, however, that the natural energy decomposition analysis[9] formulated within the NBO scheme does provide an energetic description of an interaction between two fragments. For weak interactions, when no NBO or no bond path is found, they hardly deliver any meaningful information. A simple alternative of these methods are various bond-order schemes.[10–15] Their advantage is that a characteristic value (bond order or bond index) is attributed to each pair of atom in a molecule. Thus, the bond order is a continuous measure of bonding, available at any molecular configuration. The most widely used bond-order scheme is due to Mayer,[13,14] which is essentially a generalization of Wiberg bond indices[12] for the case of nonorthogonal basis functions. Since the Mayer bond orders are easy to evaluate and to interpret, they are frequently used to elucidate molecular structures. Some drawbacks should be also mentioned. The bond orders do not allow distinguishing between weak attractive and repulsive interactions, as they are almost always positive (Mayer bond orders may sometimes exhibit very low negative values, whereas Wiberg bond indices are nonnegative by construction). Another problem is that a significant bond order is obtained for terminal atoms involved into a three-center bond even in the absence of direct overlap between them. This artifact is caused by the mathematical

construction of bond orders.[16] Finally, in spite of all its merits, bond orders by no means provide an energetic measure of an interatomic interaction.

Another approach to the bond energetics within a molecule is to *decompose* the total energy of the molecule (within a given quantum-chemical method) into a sum of monoatomic and diatomic contributions as follows:

$$E = \sum_A E(A) + \sum_{A>B} E(AB) = \sum_A E(A) + \frac{1}{2}\sum_{A\neq B} E(AB). \quad (3)$$

Such a partitioning is not unique. It is rather simple for semiempirical methods[17] but no longer trivial for *ab initio* methods due to the presence of four-center two-electron integrals in the total energy expression.

A very useful energy partitioning technique for the Hartree–Fock energy in the Hilbert space of atomic orbitals, called "chemical energy component analysis," was proposed by Mayer and co-worker,[18,19] who made use of one-atom projection operators. Later, Mayer[20] found a simpler and eventually more efficient partitioning scheme by assigning various terms of the total Hartree–Fock energy expression to different atoms. Earlier, Ichikawa and Yoshida[21] proposed a very similar, though not identical, method. The Mayer and Ichikawa–Yoshida methods differ in the treatment of the exchange term. However, recently, it has been shown that the Ichikawa–Yoshida scheme exhibits serious problems in some cases, while yielding results similar to the Mayer scheme in the others.[22] Another Hartree–Fock energy partitioning was proposed by Nakai and Kikuchi.[23]

Vyboishchikov *et al.*[24] generalized the Mayer partitioning scheme for the case of density-functional theory (DFT). In this approach the exchange-correlation energy density per electron ε_{xc} is expanded into a linear combination of atom-centered basis functions, while other terms of the energy expression are treated in the same way as in Mayer's method. It should be noted that this method of the DFT energy partitioning is not identical to Mayer's Hartree–Fock partitioning even if ε_{xc} were equivalent to the Hartree–Fock exchange.

Recently, Vyboishchikov and Salvador[25] have introduced a technique for the total energy partitioning for an arbitrary correlated *ab initio* method using the cumulant representation of the second-order density matrix. Alternatively, it is possible to partition the correlation energy separately using the Nesbet theorem[26] as proposed by Ayala and Scuseria.[27] Thus, the decomposition of the total energy using the same principles is now available both at Hartree–Fock, DFT, and correlated *ab initio* levels.

In addition to the above mentioned schemes that use the energy partitioning in the Hilbert space, there exists a group of methods, in which the partitioning is done in the three-dimensional physical space of the molecule.[28–33]

The two energy decomposition approaches discussed above, the fragment-based methods (such as Ziegler–Rauk and Kitaura–Morokuma) and the diatomic energy methods (such as Mayer's), tackle the question about the nature of the chemical bond from opposite ends. The Ziegler–Rauk and Kitaura–Morokuma methods focus on the energetic consequences of the bond formation process, whereas the Mayer approach separates the total energy of the final molecule in several contributions without using an explicit reference. The two types of approaches should thus be considered to be complementary. It is the purpose of the present work to shed light on the relation between the two approaches and to show in which sense they are complementary.

The article is structured as follows. Section II gives the computational details. In Sec. III we discuss the Mayer scheme in more detail, paying attention to the properties of the one-atom density that we define below ("Mulliken density"), which is of central importance for the understanding of the energetic terms in the Mayer scheme. This atomic density also allows for a comparison of the electrostatic component of the dissociation energy (ΔE_{elstat}) that shows up in both approaches. Afterwards we discuss the results of the Mayer and the EDA energy decomposition schemes for a number of molecules at both the Hartree–Fock and DFT levels of theory. Section IV summarizes the conclusions.

II. COMPUTATIONAL DETAILS

The Hartree–Fock geometry optimization and the evaluation of molecular orbitals needed for our calculations were performed at the RHF level using the GAUSSIAN 03 program package[34] with the standard 6–31G** basis set with Cartesian polarization functions. Analogous density-functional calculations were done using the conventional BP86 functional.[35,36] The Hartree–Fock diatomic energy components were calculated according to formula (8), while for the DFT diatomic energies, Eqs. (12)–(14) from Ref. 24 were employed. FORTRAN codes written by the authors were used.

For the Ziegler–Rauk energy decomposition analysis, a locally modified version of the GAUSSIAN 03 program was used. The wave functions for open-shell fragments were obtained within the restricted open-shell formalism.

III. RESULTS AND DISCUSSION

A. Mayer's Hartree–Fock energy partitioning

In the previous publications, we demonstrated that Mayer's Hartree–Fock energy partitioning[20] can be easily rederived using the following approach.[24,25] First, the total unrestricted Hartree–Fock energy expression is written in terms of electron density and density matrix as follows (real spin-orbitals will be considered throughout the paper):

$$E^{\text{HF}} = \sum_{A>B} \frac{Z_A Z_B}{R_{AB}} + \sum_{\mu,\nu} D_{\mu\nu}[\nu|\hat{T}|\mu] - \sum_A \int \frac{Z_A}{r_A}\rho(\mathbf{x})d\mathbf{x} + \frac{1}{2}\int\int \frac{\rho(\mathbf{x})\rho(\mathbf{x}')}{|\mathbf{r}-\mathbf{r}'|}d\mathbf{x}d\mathbf{x}' - \frac{1}{2}\int\int \frac{\rho(\mathbf{x}|\mathbf{x}')\rho(\mathbf{x}'|\mathbf{x})}{|\mathbf{r}-\mathbf{r}'|}d\mathbf{x}d\mathbf{x}'. \quad (4)$$

Here $\mathbf{x}$ stands for the spatial coordinates $\mathbf{r}$ and spin coordinates ω of an electron, $D_{\mu\nu}$ is an element of the charge-density bond-order matrix in a real spin-orbital basis, and

$\rho(\mathbf{x})$ and $\rho(\mathbf{x}|\mathbf{x}')$ are *density* and *density matrix* functions, respectively,

$$\rho(\mathbf{x}|\mathbf{x}') = \sum_{\mu,\nu}^{\text{all}} D_{\mu\nu}\chi_\nu(\mathbf{x})\chi_\mu(\mathbf{x}'),$$
$$\rho(\mathbf{x}) = \rho(\mathbf{x}|\mathbf{x}) = \sum_{\mu,\nu}^{\text{all}} D_{\mu\nu}\chi_\nu(\mathbf{x})\chi_\mu(\mathbf{x}). \tag{5}$$

If, in some manner, the total densities $\rho(\mathbf{x})$ and $\rho(\mathbf{x}|\mathbf{x}')$ can be separated into atomic contributions as follows:

$$\rho(\mathbf{x}) = \sum_A \rho^A(\mathbf{x}),$$
$$\rho(\mathbf{x}|\mathbf{x}') = \sum_A \rho^A(\mathbf{x}|\mathbf{x}');$$

then the Hartree–Fock energy expression can be rearranged as follows ($\hat{T}$ is the kinetic energy operator):

$$E^{\text{HF}} = \sum_{AB}\sum_{\mu\in A}\sum_{\nu\in B} D_{\mu\nu}[\nu|\hat{T}|\mu] + \sum_{A>B}\frac{Z_A Z_B}{R_{AB}} - \sum_{AB}\int\frac{Z_B}{r_B}\rho^A(\mathbf{x})d\mathbf{x} + \frac{1}{2}\sum_{AB}\int\int\frac{\rho^A(\mathbf{x})\rho^B(\mathbf{x}')}{|\mathbf{r}-\mathbf{r}'|}d\mathbf{x}d\mathbf{x}' - \frac{1}{2}\sum_{AB}\int\int\frac{\rho^A(\mathbf{x}|\mathbf{x}')\rho^B(\mathbf{x}'|\mathbf{x})}{|\mathbf{r}-\mathbf{r}'|}d\mathbf{x}d\mathbf{x}', \tag{6}$$

which gives rise to monoatomic and diatomic components of the Hartree–Fock energy

$$E^{\text{HF}}(A) = \sum_{\mu,\nu\in A} D_{\mu\nu}[\nu|\hat{T}|\mu] - \int\frac{Z_A}{r_A}\rho^A(\mathbf{x})d\mathbf{x} + \frac{1}{2}\int\int\frac{\rho^A(\mathbf{x})\rho^A(\mathbf{x}')}{|\mathbf{r}-\mathbf{r}'|}d\mathbf{x}d\mathbf{x}' - \frac{1}{2}\int\int\frac{\rho^A(\mathbf{x}|\mathbf{x}')\rho^A(\mathbf{x}'|\mathbf{x})}{|\mathbf{r}-\mathbf{r}'|}d\mathbf{x}d\mathbf{x}', \tag{7}$$

$$E^{\text{HF}}(AB) = 2\sum_{\mu\in A}\sum_{\nu\in B} D_{\mu\nu}[\nu|\hat{T}|\mu] + \left(\frac{Z_A Z_B}{R_{AB}} - \int\frac{Z_B}{r_B}\rho^A(\mathbf{x})d\mathbf{x} - \int\frac{Z_A}{r_A}\rho^B(\mathbf{x})d\mathbf{x} + \int\int\frac{\rho^A(\mathbf{x})\rho^B(\mathbf{x}')}{|\mathbf{r}-\mathbf{r}'|}d\mathbf{x}d\mathbf{x}'\right) - \int\int\frac{\rho^A(\mathbf{x}|\mathbf{x}')\rho^B(\mathbf{x}'|\mathbf{x})}{|\mathbf{r}-\mathbf{r}'|}d\mathbf{x}d\mathbf{x}'. \tag{8}$$

The term in parentheses in Eq. (8) represents the Coulomb interaction (ΔE_{elstat}) between the one-atom electron densities and nuclei of atoms A and B, while the last term is the exchange interaction (ΔE_{ex}). Both terms are expressed through the one-atom density and density matrix. However, the kinetic energy partitioning cannot be represented through the one-atom densities.

Upon introducing a specific definition of a *one-atom density matrix* function $\rho^A(\mathbf{x}|\mathbf{x}')$ and a *one-atom density* $\rho^A(\mathbf{x})$ as follows:[24,25,37]

$$\rho^A(\mathbf{x}|\mathbf{x}') = \sum_{\mu\in A}^{\text{all}}\sum_{\nu} D_{\mu\nu}\chi_\nu(\mathbf{x})\chi_\mu(\mathbf{x}'),$$
$$\rho^A(\mathbf{x}) = \rho^A(\mathbf{x}|\mathbf{x}) = \sum_{\mu\in A}^{\text{all}}\sum_{\nu} D_{\mu\nu}\chi_\nu(\mathbf{x})\chi_\mu(\mathbf{x}), \tag{9}$$

which we refer to as "Mulliken" densities, and inserting the expressions of $\rho^A(\mathbf{x})$ and $\rho^A(\mathbf{x}|\mathbf{x}')$ from Eq. (9) into Eq. (4), a Hartree–Fock energy partitioning results, which is exactly coincident with that originally formulated by Mayer in terms of molecular integrals.[20]

Essentially, the qualitative picture of chemical bonding in Mayer's method[20] and its generalizations[24,25] is as follows. When a free atom A with a total energy $E_0(A)$ is inserted into a molecule, it is *promoted* to an energy $E(A)$. The difference $E_{\text{def}}(A)=E(A)-E_0(A)$ is called promotion or deformation energy. In fact, it describes not only the promotion but also other changes such as electron transfer. Afterward, the atoms interact with each other to give rise to pairwise diatomic *interaction* energies $E(AB)$ [see Eq. (3)]. Thus, the diatomic energy is not equivalent to the dissociation energy, even in the case of a diatomic molecule, because both diatomic and one-atom promotion energies contribute to the dissociation energy. Quantitatively, this simple idea can be demonstrated for the case of a diatomic molecule AB as follows:

$$\begin{aligned} E^{\text{HF}}_{\text{diss}}(AB) &= E^{\text{HF}}_0(AB) - E^{\text{HF}}_0(A) - E^{\text{HF}}_0(B) \\ &= E^{\text{HF}}(A) + E^{\text{HF}}(B) + E^{\text{HF}}(AB) - E^{\text{HF}}_0(A) - E^{\text{HF}}_0(B) \\ &= (E^{\text{HF}}(A) - E^{\text{HF}}_0(A)) + (E^{\text{HF}}(B) - E^{\text{HF}}_0(B)) \\ &\quad + E^{\text{HF}}(AB) \\ &= E^{\text{HF}}_{\text{def}}(A) + E^{\text{HF}}_{\text{def}}(B) + E^{\text{HF}}(AB). \end{aligned}$$

A similar connection to the dissociation energies was presented by Martín Pendás *et al.*[38] within their own decomposition scheme.

The diatomic energy $E^{\text{HF}}(AB)$ can be divided into kinetic E_{kin}, electrostatic E_{elst}, and exchange E_{ex} energy components as follows:

$$E^{\text{HF}}(AB) = E_{\text{kin}}(AB) + E_{\text{elst}}(AB) + E_{\text{ex}}(AB). \tag{10}$$

The kinetic and exchange energy components are given by the expressions

$$E_{\text{kin}}(AB) = 2\sum_{\mu\in A}\sum_{\mu\in B} D_{\mu\nu}[\nu|T|\mu],$$
$$E_{\text{ex}}(AB) = -\int\int\frac{\rho^A(\mathbf{x}|\mathbf{x}')\rho^B(\mathbf{x}'|\mathbf{x})}{|\mathbf{r}-\mathbf{r}'|}d\mathbf{x}d\mathbf{x}' = -\sum_{\mu\in A}\sum_{\rho\in B}\sum_{\sigma,\nu}^{\text{all}} D_{\mu\sigma}D_{\rho\nu}(\mu\nu|\rho\sigma).$$

The electrostatic energy can be further split into nuclear repulsion E_{NN}, electron-nuclear attraction E_{eN}, and electron-electron repulsion E_C as follows:

$$E_{\mathrm{elst}}(AB) = E_{NN}(AB) + E_{eN}(AB) + E_C(AB),$$

where

$$E_{NN}(AB) = Z_A Z_B / R_{AB},$$

$$E_{eN}(AB) = -\int \rho^A(\mathbf{x}) \frac{Z_B}{r_B} d\mathbf{x} - \int \rho^B(\mathbf{x}) \frac{Z_A}{r_A} d\mathbf{x},$$

$$E_C(AB) = \int\int \frac{\rho^A(\mathbf{x})\rho^B(\mathbf{x}')}{|\mathbf{r}-\mathbf{r}'|} d\mathbf{x} d\mathbf{x}' = \sum_{\mu\in A}\sum_{\rho\in B}\sum_{\nu,\sigma}^{\text{all}} D_{\mu\nu} D_{\rho\sigma} (\mu\nu|\rho\sigma). \quad (11)$$

Although the above formulas are written for a diatomic molecule AB, they would remain valid if the notations A and B referred to fragments of a polyatomic molecule rather than to atoms in a diatomic one.

B. Mulliken densities

The comparison of Eq. (10) with Eq. (1a) and especially of Eq. (8) with Eq. (2) shows the close resemblance of the electrostatic energy terms in both schemes. The difference comes solely from the densities $\rho^{A,B}$ used in the expressions. In the EDA scheme, undisturbed densities of the free atoms (in the case of diatomic molecules) are employed, whereas in the Mayer scheme, the one-atom Mulliken densities ρ^A appear. The latter can be seen as those resulting when all interactions in the molecule are taken into account, since they sum to the total molecular density. Taking the perspective of bond formation, the densities in the EDA scheme could be referred to as *starting* densities and those in the Mayer as the *final* densities. These densities are of course identical only for very large atomic separations. A detailed analysis of the one-atom Mulliken densities $\rho^A(\mathbf{x})$ defined according to Eq. (9) can give useful insight for the comparative discussion in Sec. IIID.

The one-atom Mulliken density $\rho^A(\mathbf{x})$ has an important property of giving the Mulliken atomic population when integrated over the entire space as follows:

$$N_A = \int \rho^A(\mathbf{x}) d\mathbf{x} = \sum_{\mu\in A}\sum_{\nu}^{\text{all}} D_{\mu\nu} \int \chi_\nu(\mathbf{x})\chi_\mu(\mathbf{x}) d\mathbf{x} = \sum_{\mu\in A}\sum_{\nu}^{\text{all}} D_{\mu\nu} S_{\nu\mu} = \sum_{\mu\in A} (DS)_{\mu\mu}.$$

It is for this reason that we refer to them as Mulliken densities. They are related to the one-atom "operator of the number of electrons" used by Mayer within the second-quantization formalism.[14] The one-atom density matrix $\rho^A(\mathbf{x}|\mathbf{x}')$ is also closely related to Mayer bond orders B_{AB} as follows:

$$B_{AB} = \int\int \rho^A(\mathbf{x}|\mathbf{x}')\rho^B(\mathbf{x}'|\mathbf{x}) d\mathbf{x} d\mathbf{x}'.$$

Therefore, the Mayer energy partitioning is consistent with the Mulliken population analysis and Mayer's bond orders. It is the Mulliken one-atom density and density matrix that provide the nexus between the three methods.

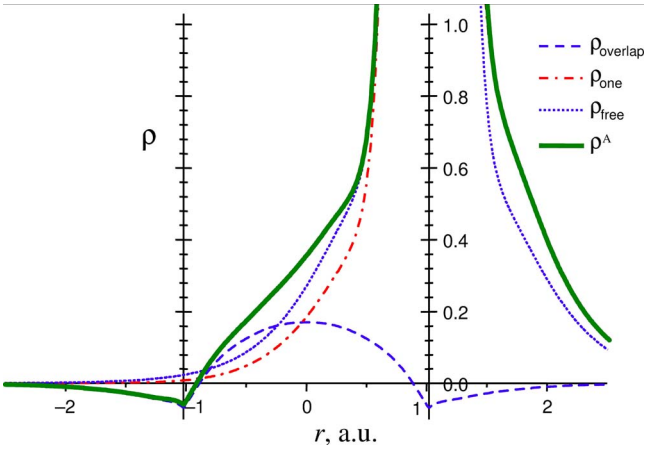

FIG. 1. (Color online) The Mulliken density ρ^N of the nitrogen atom in the N_2 molecule (bold line) and its components ρ_{one} and ρ_{overlap}. The dashed line is the free-atom density. The vertical bars indicate the positions of the nuclei.

It is important to consider the properties of the Mulliken density $\rho^A(\mathbf{x})$. First, the summation in Eq. (9) over the first index μ runs over the basis functions of the atom A, while the summation over the second index ν runs over all the basis functions. Thus, Eq. (9) does not represent a quadratic form, and the positive definiteness of the density matrix D does not necessarily result in positive values of $\rho^A(\mathbf{x})$ at an arbitrary point of space $\mathbf{x}$. Let us consider the practical consequences of this. In a diatomic molecule AB, the Mulliken density of atom A can be divided into two parts as follows:

$$\rho^A(\mathbf{x}) = \sum_{\mu\in A}\sum_{\nu}^{\text{all}} D_{\mu\nu}\chi_\nu(\mathbf{x})\chi_\mu(\mathbf{x}) = \sum_{\mu\in A}\sum_{\nu\in A} D_{\mu\nu}\chi_\nu(\mathbf{x})\chi_\mu(\mathbf{x}) + \sum_{\mu\in A}\sum_{\nu\in B} D_{\mu\nu}\chi_\nu(\mathbf{x})\chi_\mu(\mathbf{x}) = \rho_{\mathrm{one}}(\mathbf{x}) + \rho_{\mathrm{overlap}}(\mathbf{x}).$$

The first summand $\rho_{\mathrm{one}}(\mathbf{x})$ is a quadratic form and thus nonnegative. The second term is the overlap density

$$\rho_{\mathrm{overlap}}(\mathbf{x}) = \sum_{\mu\in A}\sum_{\nu\in B} D_{\mu\nu}\chi_\nu(\mathbf{x})\chi_\mu(\mathbf{x}).$$

This can be either positive or negative, in general. Of course, it is expected that ρ_{overlap} has substantial positive values in the bonding area, but this is not guaranteed in other regions of space.

To check the practical consequences of the mathematical construction of ρ^A, we plotted a graph of it and its components ρ_{one} and ρ_{overlap} along the N–N bond in the dinitrogen molecule (Fig. 1). As expected, the positive component ρ_{one} decreases monotonically from the nucleus and vanishes asymptotically at long distances. The decrease of ρ_{one} in the bonding region is faster than behind the nucleus. The overlap density has a clear maximum in the bonding area, which is due to the symmetry located in N_2 exactly at the bond midpoint. When going from the midpoint toward a nucleus, the ρ_{overlap} decreases rapidly, reaching zero at about 0.125 a.u. from the nucleus. Then, in the immediate vicinity of the nucleus, ρ_{overlap} turns negative and has a relatively sharp

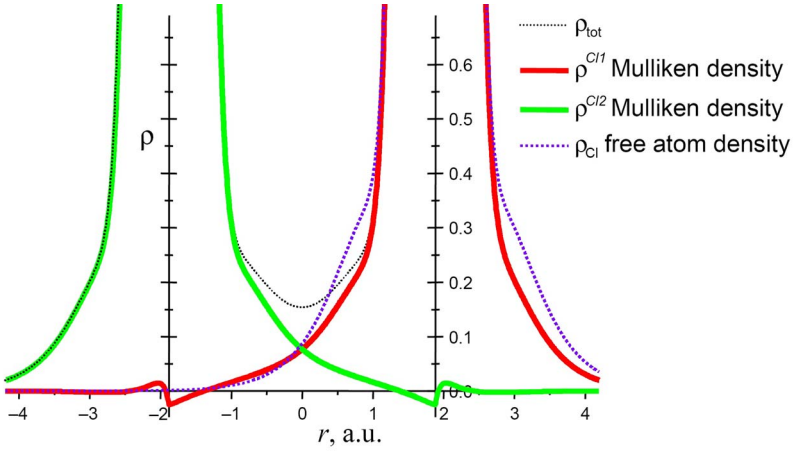

FIG. 2. (Color online) The total electron density ρ_{tot} (thin dashed curve) and Mulliken densities of each of the chlorine atoms in the Cl_2 molecule ρ^{Cl1} and ρ^{Cl2} (bold curves). The bold dashed curve is the free-atom density ρ_{Cl}. The vertical bars indicate the positions of the nuclei.

maximum near the nuclear position. Behind the nucleus, $\rho_{overlap}$ starts to decay slowly, asymptotically vanishing at infinity.

Figure 2 shows the Mulliken densities in the dichlorine molecule. Basically, it exhibits a behavior similar to the N_2 case. ρ^{Cl} vanishes and turns negative before the nucleus and reaches a minimum at the nuclear position. However, behind the nucleus, it changes the sign again but then rapidly vanishes, exhibiting another sign change. Subsequently, it gradually decays with small negative values of ρ^{Cl}. The examples of N_2 and Cl_2 indicate that the small negative areas of Mulliken densities are caused by the contribution to the overlap density of compact core orbitals, since they have different nodal structures depending on the principal quantum number.

Although the regions of negative one-atom density are rather small, it is not *a priori* clear what consequences for the diatomic energies they may have. Since they are located around the nucleus of the other atom, their contribution to the electron-nuclear interaction (which is then *repulsive*) may be considerable. In order to check this, we numerically calculated the contribution of negative one-atom density to the diatomic electron-nuclear interaction E_{eN}^{-} using the BP86 density according to the formula

$$E_{eN}^{-}(AB) = -\int_{\Omega_-(A)} \rho^A \frac{Z_B}{r_B} d\mathbf{r} - \int_{\Omega_-(B)} \rho^B \frac{Z_A}{r_A} d\mathbf{r},$$

where the integration runs over the region of negative one-atom density of the atom A $\Omega_-(A)$. For the N_2 molecule, this calculation yields $E_{eN}^{-}(AB) = +0.4968$ hartree, whereas the total diatomic electron-nuclear attraction $E_{eN}(AB)$ evaluated using Eq. (11) is −45.8740 hartree. A similar calculation for Cl_2 gives an $E_{eN}^{-}(AB)$ value of +0.6782 hartree, while the total energy $E_{eN}(AB)$ is −147.8226 hartree. Therefore, we conclude that the energetic effect of the areas of negative one-atom density is moderate, but significant.

The fact that the Mulliken density is formulated in terms of the basis functions raises the question of the basis-set dependence of Mulliken densities. To clarify this point, we plotted the Mulliken one-atom density of one of the nitrogen atoms in N_2 calculated using a number of basis sets. Substantial difference is found in the area of the other nitrogen nucleus, which is evident from Fig. 3. While for all basis sets tested, the Mulliken density turns negative somewhere around the nucleus, its exact behavior varies with the basis set. While for the basis sets containing polarization functions as well as for STO-3G, $\rho^N(r)$ has a negative maximum at the nuclear position, the other basis sets exhibit a smoother decay, with a small positive maximum or a shoulder at the nucleus. In this case, the $\rho^N(r)$ turns negative behind the nucleus.

C. Results for test molecules

1. Diatomic energy decomposition results

The diatomic energy components were calculated for the series of molecules C_2H_6, C_2H_4, C_2H_2, CO, F_2, Cl_2, N_2, NH_3BH_3, and LiH. The total diatomic interaction energies E_{tot} and its components (electrostatic, kinetic, and exchange energies) are given in Table I (Hartree–Fock values) and Table II (DFT values). We mainly discuss the values of the individual components rather than E_{tot}, since a thorough discussion of the latter and their comparison have been already given in Ref. 24.

For the bonding C–C and C–H interactions in ethane and ethylene, the DFT values for ΔE_{elstat} are quite similar at the Hartree–Fock and DFT levels. The kinetic energy component differs slightly more, and so does the Hartree–Fock exchange versus the DFT exchange-correlation component.

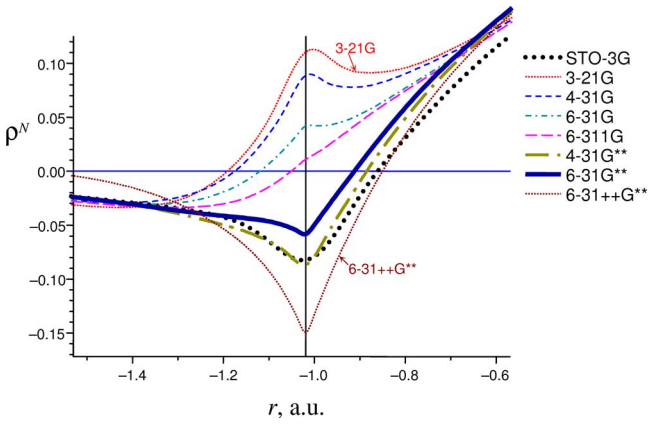

FIG. 3. (Color online) The Mulliken density ρ^N of the nitrogen atom 2 in the region of atom 1 in the N_2 molecule calculated using various basis sets.

TABLE I. Results of the Mayer Hartree–Fock energy partitioning at the RHF/6-31G** level. The total Mayer diatomic interaction energy (E_{tot}^{HF}) and its components (electrostatic, kinetic, and exchange energies) are given in kcal mol^{-1}. Group interaction energies, defined as the sum of the diatomic interaction energies between two given groups of atoms, are given in italics. Dissociation energy D_e and preparation energy E_{prep} are also given.

	ΔE_{elstat}	ΔE_{kin}	ΔE_{ex}	E_{tot}^{HF}	E_{prep}	D_e
C_2H_6						
C–C	−137.1	238.9	−220.8	−119.0		
C–H	−138.3	246.0	−215.7	−108.0		
C···H	1.1	−3.2	6.5	4.4		
H···H^{gem}	5.6	−2.1	5.0	8.6		
H···H^{anti}	1.2	−1.5	−0.3	−0.6		
H···H^{gauch}	1.7	0.6	0.5	2.8		
CH_3–CH_3	−116.3	*219.0*	−180.1	−77.4	*8.8*	*68.6*
C_2H_4						
C=C	−244.3	489.1	−411.7	−166.8		
C–H	−138.6	245.5	−218.2	−111.4		
C···H	2.5	−3.7	7.3	6.1		
H···H^{gem}	6.3	−0.9	5.5	11.0		
H···H^{trans}	1.4	−1.2	−0.4	−0.2		
H···H^{cis}	2.4	0.9	0.6	3.9		
CH_2–CH_2	−226.6	*473.6*	−381.9	−135.0	*17.1*	*117.9*
C_2H_2						
C≡C	−405.0	771.1	−670.7	−304.6		
C–H	−126.4	228.8	−200.8	−98.4		
C···H	−10.6	1.4	−2.7	−11.9		
H···H	4.7	−0.9	−0.3	3.5		
CH–CH	−421.6	*773.0*	−676.4	−324.9	*158.6*	*166.3*
CO						
C–O	−384.8	878.7	−564.6	−70.8	−100.1	171.4
F_2						
F–F	−112.8	210.3	−200.5	−103.0	70.3	32.7
Cl_2						
Cl–Cl	−34.2	65.4	−123.8	−92.6	82.0	10.6
N_2						
N–N	−413.2	1003.4	−652.1	−61.9	−46.7	108.6
NH_3BH_3						
B–N	−126.4	100.8	−93.1	−118.7		
B–H	−117.4	199.1	−190.8	−109.1		
N···H	20.0	0.6	3.3	23.9		
H···H(B)	6.9	−0.01	2.7	9.6		
B···H	19.9	−1.5	2.4	20.8		
H(N)···H(B)^{anti}	−5.7	−1.0	−0.2	−6.9		
H(N)···H(B)^{gauche}	−6.9	0.4	0.3	−6.2		
N–H	−195.6	275.8	−217.7	−137.5		
H···H(N)	22.1	−1.3	3.4	24.2		
NH_3–BH_3	−65.0	*97.4*	−75.2	−42.8	*19.9*	*22.9*
LiH						
Li–H	−52.2	91.2	−130.6	−91.6	59.1	32.5

In the case of acetylene, all three Hartree–Fock components are larger in absolute value than their DFT counterparts. This is obviously a consequence of a geometry change, as the C≡C triple bond is more contracted at the Hartree–Fock than at the BP86 level.

In the CO, F_2, and N_2 molecules (but not in Cl_2), the situation is qualitatively similar to that in acetylene. That is, the absolute values of all components are higher in the Hartree–Fock case. For the NH_3BH_3 molecule, the total N–B diatomic energy at the BP86 level is very close to that in

TABLE II. Results of the DFT energy partitioning at the BP86/6-31G** level. The total diatomic interaction energy (E_{tot}^{DFT}) and its components (electrostatic, kinetic, and exchange energies) are given in kcal mol^{-1}. Group interaction energies are given in italics. Dissociation energy D_e and preparation energy E_{prep} are also given.

	ΔE_{elstat}	ΔE_{kin}	ΔE_{ex}	E_{tot}^{DFT}	E_{prep}	D_e
C_2H_6						
C–C	−139.2	240.3	−176.3	−75.2		
C–H	−132.7	225.2	−215.1	−122.6		
C···H	−0.6	−2.3	−6.8	−9.8		
H···H^{gem}	6.0	−1.9	−7.7	−3.6		
H···H^{anti}	1.5	−1.8	−0.2	−0.5		
H···H^{gauch}	2.0	0.8	−1.2	1.7		
CH_3–CH_3	−126.4	*226.0*	−224.8	−125.1	*27.5*	*97.6*
C_2H_4						
C=C	−243.8	466.4	−391.3	−168.6		
C–H	−127.6	219.6	−208.7	−116.7		
C···H	2.0	−2.2	−6.9	−7.1		
H···H^{gem}	7.0	−1.3	−0.1	5.7		
H···H^{trans}	1.2	−2.0	−0.1	−1.0		
H···H^{cis}	2.3	1.7	0.2	4.1		
CH_2–CH_2	−229.1	*457.1*	−418.7	−190.7	*10.6*	*180.1*
C_2H_2						
C≡C	−351.3	676.8	−594.6	−269.1		
C–H	−118.8	207.8	−209.0	−120.0		
C···H	1.2	2.6	−8.5	−4.8		
H···H	2.1	−0.9	−0.1	1.1		
CH–CH	−346.8	*681.0*	−611.8	−277.5	*9.0*	*268.5*
CO						
C–O	−323.0	754.4	−537.3	−105.9	−160.2	266.1
F_2						
F–F	−86.9	153.2	−144.3	−78.0	20.3	57.7
Cl_2						
Cl–Cl	−41.8	59.9	−188.7	−170.7	114.0	56.7
N_2						
N–N	−342.7	815.8	−607.0	−133.8	−98.5	232.3
NH_3BH_3						
B–N	−100.9	136.1	−108.6	−73.4		
B–H	−105.9	190.9	−181.0	−96.0		
N–H	−173.4	244.9	−234.8	−163.3		
H···H(B)	3.6	0.3	−10.1	−6.2		
N···H	11.5	1.0	−11.4	1.0		
B···H	7.7	−2.5	−2.0	3.2		
H(N)···H(B)^{anti}	−3.4	−1.4	−0.1	−4.9		
H(N)···H(B)^{gauche}	−4.0	0.4	−1.2	−4.9		
H···H(N)	20.7	−1.4	−4.7	14.6		
NH_3–BH_3	−77.5	*130.0*	−157.1	−104.6	*68.7*	*35.9*
LiH						
Li–H	−51.2	87.3	−123.3	−87.1	29.9	57.2

C_2H_6. However, the individual components in both isoelectronic molecules are very different. All three components ΔE_{elstat}, ΔE_{kin}, and ΔE_{ex} are lower in absolute value in NH_3BH_3 than in C_2H_6. Notably, $\Delta E_{kin}+\Delta E_{ex}$ together are about 37 kcal mol^{-1} more positive in NH_3BH_3, but the electrostatics is about 38 kcal mol^{-1} more favorable in C_2H_6. The group interaction energy for CH_3-CH_3 is 20 kcal mol^{-1} higher than for NH_3-BH_3. The difference comes largely from electrostatics, although NH_3BH_3 has also a significantly attractive value for $\Delta E_{kin}+\Delta E_{ex}$. The preparation energy for

TABLE III. Results of the Ziegler–Rauk EDA at HF/6-31G**. All energies are in kcal mol^{-1}. The following fragmentations were chosen: N–N in the case of N_2, Li–H in LiH, H_3C-CH_3 in C_2H_6, H_2C-CH_2 in C_2H_4, HC–CH in C_2H_2, and H_3N-BH_3 in NH_3BH_3. The values in parentheses are percentage contributions to the total attractive interactions $\Delta E_{\text{elstat}}+\Delta E_{\text{orb}}$.

	ΔE_{int}	ΔE_{Pauli}	ΔE_{elstat}	ΔE_{orb}	ΔE_{prep}	D_e
C_2H_6	−85.4	235.6	−139.2 (43%)	−181.9 (57%)	16.8	68.9
C_2H_4	−122.7	396.0	−195.8 (38%)	−322.9 (62%)	4.8	117.9
C_2H_2	−166.5	494.5	−155.0 (23%)	−506.0 (77%)	0.2	166.3
N_2	−108.6	1069.0	−343.2 (29%)	−834.4 (71%)	0.0	108.6
NH_3BH_3	−36.7	98.9	−86.7 (64%)	−48.8 (36%)	13.8	22.9
LiH[a]	−32.5	32.9	−7.7 (12%)	−57.7 (88%)	0.0	32.5
LiH[b]	−202.9	29.2	−202.9 (87%)	−29.2 (13%)	170.4	32.5

[a]Taking Li^0 and H^0 as reference fragments.
[b]Taking Li^{+1} and H^{-1} as reference fragments.

NH_3-BH_3 is much higher than for C_2H_6. This is sensible because the electronic changes in NH_3BH_3 are more pronounced and include charge transfer.

2. Ziegler–Rauk energy decomposition results

The results of the EDA for the series of test molecules are given in Tables III and IV at the Hartree–Fock and the BP86 DFT level of theory, respectively.

The electrostatic component to the interaction energy ΔE_{elstat} is quite similar in both the Hartree–Fock and the DFT calculations for all systems. This manifests the fact that the charge distributions of the fragments resulting from a Hartree–Fock and a DFT calculation do not differ considerably. The ΔE_{Pauli} and ΔE_{orb} terms on the other hand deviate quite substantially for all systems between the Hartree–Fock and DFT levels of theory. The absolute value of the ΔE_{Pauli} and the ΔE_{orb} terms is always considerably larger in the Hartree–Fock case, except for LiH and BH_3NH_3. Interestingly, the relative importance of the electrostatic term ΔE_{elstat} and the orbital term ΔE_{orb} to the stabilizing contributions of the interaction energy $\Delta E_{\text{elstat}}+\Delta E_{\text{orb}}$ is quite similar at the Hartree–Fock and DFT levels (see the values in parentheses in Tables III and IV). The largest deviation is observed for C_2H_2. This means that the bonding picture is similar at the Hartree–Fock and DFT levels.

Here we will not discuss the different components in detail, since this has already been done in previous publications[39,40] focusing instead on the comparison between the Mayer and the EDA scheme at the DFT level.

TABLE IV. Results of the Ziegler–Rauk EDA at the BP86/6-31G** level. Energies are given in kcal mol^{-1}. The following fragmentations were chosen: N–N in the case of N_2, Li–H in LiH, H_3C-CH_3 in C_2H_6, H_2C-CH_2 in C_2H_4, HC–CH in C_2H_2, and H_3N-BH_3 in NH_3BH_3. The values in parentheses are percentage contributions to the total attractive interactions $\Delta E_{\text{elstat}}+\Delta E_{\text{orb}}$.

	ΔE_{int}	ΔE_{Pauli}	ΔE_{elstat}	ΔE_{orb}	ΔE_{prep}	D_e
C_2H_6	−114.4	187.2	−137.0 (45%)	−164.6 (55%)	16.8	97.6
C_2H_4	−185.6	273.4	−188.7 (41%)	−270.3 (59%)	5.5	180.1
C_2H_2	−268.7	268.1	−149.8 (28%)	−387.1 (72%)	0.2	268.5
N_2	−232.3	767.5	−311.2 (31%)	−688.6 (69%)	0.0	232.3
NH_3BH_3	−48.6	100.3	−89.7 (60%)	−59.2 (40%)	12.7	35.9
LiH[a]	−57.1	16.5	−7.8 (11%)	−65.8 (89%)	0.0	57.2
LiH[b]	−208.3	28.4	−202.7 (86%)	−33.9 (14%)	151.1	57.2

[a]Taking Li^0 and H^0 as reference fragments.
[b]Taking Li^{+1} and H^{-1} as reference fragments.

3. Comparison

A recent EDA study[39,40] on the nature of the chemical bond in a number of nonpolar, strongly bound molecules such as N_2 highlighted the importance of the electrostatic contribution ΔE_{elstat} even in such systems that are traditionally discussed solely on the basis of covalent contributions. In N_2 this electrostatic contribution amounts to -311.2 kcal mol^{-1}, which corresponds to one-third of the overall stabilizing contributions ($\Delta E_{elstat}+\Delta E_{orb}$) to the interaction energy. Taking into account the large Pauli repulsion ($\Delta E_{Pauli}=767.5$ kcal mol^{-1}), we note that the N_2 molecule would be unbound if the electrostatic contribution were neglected. However, as discussed above, as well as in Refs. 39 and 40, the electron density used to calculate the electrostatic contribution is the unaltered fragment density. Since density deformation will undoubtedly take place upon bond formation, the question about the electrostatic interaction energy between the deformed fragments was discussed in Refs. 39 and 40, but no clear definition of the deformed fragment densities and thus no numerical value for this energy component were given. In the case of the Mayer analysis, Eq. (9) offers a definition of a fragment density in a molecule (or at least one possible definition). The value of ΔE_{elstat} calculated for the N_2 molecule according to this definition is -342.7 kcal mol^{-1}, which is even larger than the EDA value of -311.2 kcal mol^{-1}, confirming the reasoning in Refs. 39 and 40. The kinetic term in the Mayer analysis (ΔE_{kin}) reflects the increase in the kinetic energy due to bond formation. It is related to the Pauli term (ΔE_{Pauli}) in the EDA, which has been shown to be dominated by kinetic energy contributions.[4] In the N_2 molecule both terms are very large and repulsive ($\Delta E_{kin}=815.8$ kcal mol^{-1}; $\Delta E_{Pauli}=767.5$ kcal mol^{-1}). They are counterbalanced by the electrostatic contribution and the quantum mechanical exchange (+ correlation) term in the Mayer scheme, and by the orbital term in the EDA. Interestingly, within the Mayer scheme, the N–N interaction in N_2 would also be repulsive without the electrostatic energy. Both analysis schemes lead to the description of the strong nonpolar bond in N_2 as a result of a strong charge delocalization between two centers, which is of quantum mechanical origin (ΔE_{ex} and ΔE_{orb}), and a classical electrostatic attraction between the two neutral atoms. The latter is responsible for about 30% of the overall stabilization.

For the analysis of the polar diatomic LiH molecule in the framework of the EDA, the final results are affected by the choice of the interacting fragments. Either two neutral atoms Li+H in their ^2S ground states, or two ions $Li^+ + H^-$ can be chosen. The actual polarity of the bond is not well reflected in either fragmentation, since the Mulliken analysis suggests a $Li^{+0.2}+H^{-0.2}$ decomposition. As a consequence, the EDA orbital term will include a charge-transfer contribution, which cannot be separated from the delocalization contribution. In the Mayer analysis, the charge transfer is completely included in the preparation energy and the diatomic interaction energy reflects the interaction between $Li^{+0.2}+H^{-0.2}$. This preparation process (starting from two neutral atoms) leads to an energy contribution of $E_{prep}=29.9$ kcal mol^{-1}. This can be compared to the energy needed for a complete transfer of one electron from Li to H of 151.1 kcal mol^{-1}, which is the preparation energy for the second EDA for LiH in Table IV. Taking the two EDA analyses and the Mayer analysis together one can get a more complete picture of the bonding situation, since the EDA delivers a framework in which the limiting possibilities of no or complete charge transfer are used as reference whereas the Mayer analysis considers the actual charge distribution. The amount of the electrostatic contribution ΔE_{elstat} in the three analyses reflects the complementarity of the EDA and Mayer schemes, as the EDA for Li^0+H^0 gives $\Delta E_{elstat}=-7.8$ kcal mol^{-1}, the EDA for $Li^{+1}+H^{-1}$ gives $\Delta E_{elstat}=-202.7$ kcal mol^{-1}, and the Mayer analysis gives $\Delta E_{elstat}=-51.2$ kcal mol^{-1}.

In the series C_2H_6, C_2H_4, C_2H_2, the C–C bond changes from single to double to triple bond. As has been shown before for neutral nonpolar molecules, the electrostatic contribution to the interaction energy is an important stabilizing term. Interestingly, the importance of ΔE_{elstat} in the EDA goes as $C_2H_6<C_2H_2<C_2H_4$, whereas in the Mayer approach it increases when passing $C_2H_6<C_2H_4<C_2H_2$. The deviation in the absolute values between the EDA and the Mayer analysis increases continuously from C_2H_6 over C_2H_4 to C_2H_2. Obviously, a quite dramatic charge deformation, which is stabilizing in nature, takes place upon bond formation in the case of the multiply bonded systems. This can be easily rationalized, since in a triply bonded system the charge accumulation in the bond region is more pronounced than in a singly bonded one as can be seen in deformation density plots of C_2H_2, C_2H_4, and C_2H_6 (Fig. 4). As a consequence of the quite different fragment charge distributions, on which the EDA and the Mayer analyses are based, the remaining terms of the interaction energy differ considerably as well. Nevertheless, in both schemes, the increase in the bond multiplicity leads to an increase in the absolute value of the stabilizing quantum mechanical terms (ΔE_{ex} and ΔE_{orb}), emphasizing that the bond covalency is enhanced.

The complex BH_3NH_3 serves an example of a typical donor-acceptor compound. As in the case of LiH, the charge transfer between the interacting fragments BH_3 and NH_3 is accounted for in the preparation energy in the case of the Mayer analysis, whereas in the EDA scheme the charge transfer is included in the orbital term. The Mulliken analysis gives the following charge distribution: $NH_3^{+0.33}$ and $BH_3^{-0.33}$. As a consequence, the preparation energy in the Mayer scheme ($E_{prep}=68.7$ kcal mol^{-1}) is much higher than in the EDA ($E_{prep}=12.7$ kcal mol^{-1}). Interestingly, the electrostatic term ΔE_{elstat} becomes smaller once the deformation is taken into account: In the Mayer scheme $\Delta E_{elstat}=-77.5$ kcal mol^{-1}, whereas the EDA yields $\Delta E_{elstat}=-89.7$ kcal mol^{-1}. The other energy terms are quite different as the reference charge distributions differ.

IV. SUMMARY

In this paper we critically discuss and compare two different energy decomposition schemes. The Mayer method decomposes the total energy of a molecule in monoatomic and diatomic components and can thus be used in the cases

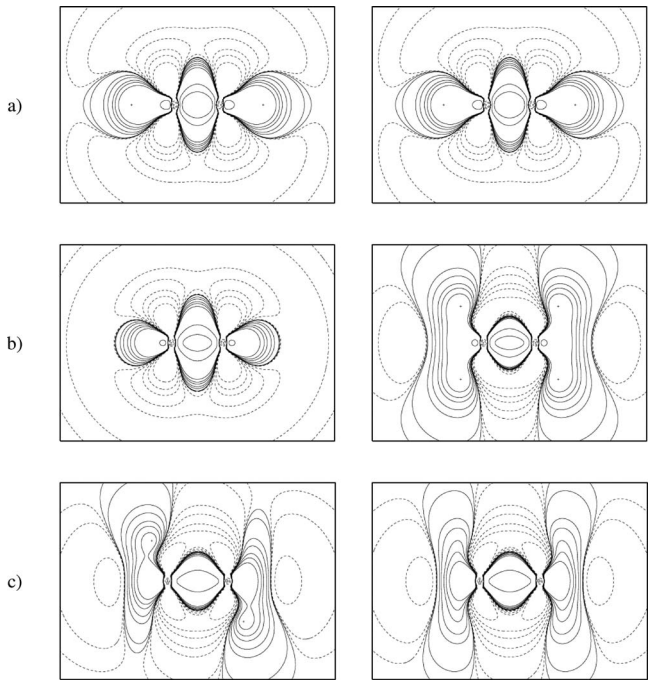

FIG. 4. The deformation electron density $\delta\rho=\rho_{\text{molecule}}-\rho_{\text{promolecule}}$ in the xz-plane (left) and in the yz-plane (right) for (a) C_2H_2 (with respect to CH fragments in the $^4\Sigma$ state), (b) C_2H_4 (with respect to CH_2 fragments in the $^3B_1$ state), and (c) C_2H_6 (with respect to CH_3 fragments in the $^2A_1$ state). The dashed lines indicate the areas of charge depletion ($\delta\rho<0$) and the solid lines show charge accumulation ($\delta\rho>0$). The contour lines are given for the following values: ±0.001, ±0.002, ±0.005, ±0.01, ±0.02, ±0.05, ±0.1, ±0.2, ±0.5, and 0.0 e bohr^{-3}.

where a fragmentation of the system in clearly separable parts is not possible. The second energy decomposition method by Ziegler and Rauk is based on a clear-cut separation of a molecule into fragments. The two methods are complementary since the first one focuses on the energy of the finally formed molecule, whereas the second one concentrates on the bond formation process starting from undeformed fragment densities. In the Mayer scheme, the density changes from the free-fragment density to the Mulliken density; subsequently, the Mulliken densities interact to give rise to the diatomic interaction energy.

We performed a detailed analysis of the diatomic energy contributions in the Mayer scheme and gave a close look on the one-atom Mulliken densities. We found that the Mulliken densities ρ^A have a large single maximum around the nuclear position of the atom A, but exhibit slightly negative values in the vicinity of neighboring atoms. The mathematical origin for the negative density is the behavior of the *overlap* density, which often has negative areas near the nuclear positions. The negative areas make a non-negligible contribution to the diatomic component of the electron-nuclear interaction.

The electrostatic energy is the main connecting point between the Ziegler–Rauk and the Mayer analyses. In both decomposition schemes electrostatic components to the interaction energy are introduced, which differ only in the definition of the fragment densities. In the Mayer scheme, the electrostatic component emerges from the interaction of the Mulliken densities, while in the Ziegler–Rauk scheme, it is the undisturbed fragment densities that interact with each other and with the nuclei. Taking the perspective of bond formation, the densities in the EDA scheme could be referred to as *starting* densities and those in the Mayer as the *final* densities. The two schemes thus allow for a complementary description of the bonding situation. The electrostatic energy components resulting from the two schemes may differ significantly. Nevertheless, they typically have the same order of magnitude.

The results of the EDA and the Mayer analysis for N_2 underline the importance of the electrostatic contribution to the bond energy even in nonpolar covalently bonded systems, since in both cases the ΔE_{elstat} term is responsible for about 30% of the overall stabilizing energy contributions. Interestingly, the absolute value of the electrostatic contribution is even larger for the Mayer scheme, which considers the interaction between deformed fragment densities, than in the EDA, which is based on undisturbed fragment densities. Also in the series C_2H_6, C_2H_4, C_2H_2 the electrostatic term is an important contribution to the overall interaction energy. Interestingly, the difference between the EDA and the Mayer analysis in the ΔE_{elstat} values increases from C_2H_6 over C_2H_4 to C_2H_2. This can be rationalized by stronger charge accumulation upon bond formation in the case of the multiply bonded systems.

In the case of polar systems such as LiH it is advantageous to utilize the EDA and the Mayer analyses together. In doing so, a more complete picture of the bonding situation can be obtained. In the EDA framework, the limiting possibilities of no (Li^0+H^0) or complete ($Li^+ + H^-$) charge transfer are used as reference, whereas the Mayer analysis considers the charge distribution consistent with the Mulliken analysis ($Li^{+0.2}+H^{-0.2}$). A similar conclusion is reached for the donor-acceptor complex BH_3NH_3, since in this case the Mulliken analysis indicates a charge transfer of 0.33 electrons from NH_3 to BH_3. The Mayer scheme includes the energy contribution of this charge transfer in the preparation energy, whereas the EDA describes this effect by the orbital term ΔE_{orb}. Interestingly, the electrostatic term ΔE_{elstat} becomes lower once the deformation and the charge transfer are taken into account, as the Mayer scheme leads to a smaller absolute value for ΔE_{elstat} than the EDA.

We conclude that both Mayer and EDA schemes are very useful for analyzing the nature of chemical bonds and that the results can be understood in the light of the discussion presented here.

ACKNOWLEDGMENTS

S.F.V. thanks the Generalitat de Catalunya for funding his research stay at Marburg University within Grant No. 2007-BE-100020. A.K. thanks the HPC program of the European Union for funding his research stay at the University of Girona and for access to the computer facilities of the Barcelona Supercomputer Center in 2007.

This work is dedicated to Professor István Mayer on the occasion of his 65th birthday.

[1] K. Kitaura and K. Morokuma, Int. J. Quantum Chem. **10**, 325 (1976).
[2] T. Ziegler and A. Rauk, Inorg. Chem. **18**, 1558 (1979).

[3] A. Krapp and G. Frenking, Chem.-Eur. J. **12**, 9196 (2006).
[4] F. M. Bickelhaupt and E. J. Baerends, Rev. Comput. Chem. **15**, 1 (2000).
[5] H. Umeyama and K. Morokuma, J. Am. Chem. Soc. **99**, 1316 (1977).
[6] J. Cioslowski, in *The Encyclopedia of Computational Chemistry*, edited by P. v. R. Schleyer, N. L. Allinger, T. Clark, J. Gasteiger, P. A. Kollman, H. F. Schaefer III, and P. R. Schreiner (Wiley, Chichester, 1998), pp. 892–905.
[7] R. F. W. Bader, in *Atoms in Molecules: A Quantum Theory*, The International Series of Monographs of Chemistry, edited by J. Halpen and M. L. H. Green (Clarendon, Oxford, 1990).
[8] A. E. Reed, L. A. Curtiss, and F. Weinhold, Chem. Rev. (Washington, D.C.) **88**, 899 (1988).
[9] E. D. Glendening and A. Streitwieser, J. Chem. Phys. **100**, 2900 (1994).
[10] B. H. Chirgwin and C. A. Coulson, Proc. R. Soc. London, Ser. A **201**, 196 (1950).
[11] R. McWeeny, J. Chem. Phys. **20**, 920 (1952).
[12] K. B. Wiberg, Tetrahedron **24**, 1083 (1968).
[13] M. Giambiagi, M. S. De Giambiagi, D. R. Grempel, and C. D. Heymann, J. Chim. Phys. Phys.-Chim. Biol. **72**, 15 (1975).
[14] I. Mayer, Chem. Phys. Lett. **97**, 270 (1983).
[15] J. Cioslowski and S. T. Mixon, J. Am. Chem. Soc. **113**, 4142 (1991).
[16] I. Mayer, *Simple Theorems, Proofs, and Derivations in Quantum Chemistry* (Springer, New York, 2003), Chap. 2.4.
[17] H. Fischer and H. Kollmar, Theor. Chim. Acta **16**, 163 (1970).
[18] I. Mayer, Chem. Phys. Lett. **332**, 381 (2000).
[19] A. Hamza and I. Mayer, Theor. Chim. Acta **109**, 91 (2003).
[20] I. Mayer, Chem. Phys. Lett. **382**, 265 (2003).
[21] H. Ichikawa and A. Yoshida, Int. J. Quantum Chem. **71**, 35 (1999).
[22] S. F. Vyboishchikov, Int. J. Quantum Chem. **108**, 708 (2008).
[23] H. Nakai and Y. Kikuchi, J. Theor. Comput. Chem. **4**, 317 (2005).
[24] S. F. Vyboishchikov, P. Salvador, and M. Duran, J. Chem. Phys. **122**, 244110 (2005).
[25] S. F. Vyboishchikov and P. Salvador, Chem. Phys. Lett. **430**, 204 (2006).
[26] R. K. Nesbet, Proc. R. Soc. London, Ser. A **230**, 312 (1955).
[27] P. Y. Ayala and G. E. Scuseria, Chem. Phys. Lett. **322**, 213 (2000).
[28] P. Salvador, M. Duran, and I. Mayer, J. Chem. Phys. **115**, 1153 (2001).
[29] I. Mayer and A. Hamza, Theor. Chem. Acc. **105**, 360 (2001).
[30] D. R. Alcoba, A. Torre, L. Lain, and R. C. Bochicchio, J. Chem. Phys. **122**, 074102 (2005).
[31] A. Sierraalta and G. Frenking, Theor. Chim. Acta **95**, 1 (1997).
[32] M. A. Blanco, A. Martín Pendás, and E. Francisco, J. Chem. Theory Comput. **1**, 1096 (2005).
[33] P. Salvador and I. Mayer, J. Chem. Phys. **120**, 5046 (2004).
[34] M. J. Frisch, G. W. Trucks, H. B. Schlegel *et al.*, GAUSSIAN 03, Revision D.01, Gaussian, Inc., Pittsburgh, PA, 2003.
[35] A. D. Becke, Phys. Rev. A **38**, 3098 (1988).
[36] J. P. Perdew, Phys. Rev. B **33**, 8822 (1986).
[37] R. Carbó-Dorca and P. Bultinck, J. Math. Chem. **36**, 201 (2004).
[38] A. Martín Pendás, M. A. Blanco, and E. Francisco, J. Comput. Chem. **28**, 161 (2007).
[39] A. Kovács, C. Esterhuysen, and G. Frenking, Chem.-Eur. J. **11**, 1813 (2005).
[40] C. Esterhuysen and G. Frenking, Theor. Chem. Acc. **111**, 381 (2004).